

Research article

Relevant Physical Factors for Estimation of Volatile Organic Compounds Emissions from Floating Storage and Offloading**Chalee Seekramon, Chalor Jarusutthirak and Pawee Klongvessa****Department of Environmental Technology and Management, Faculty of Environment, Kasetsart University, Bangkok, Thailand*

Received: 23 January 2024, Revised: 21 May 2024, Accepted: 29 July 2024, Published: 17 October 2024

Abstract

Volatile organic compounds (VOCs) have harmful effects on human and the environment. Floating storage and offloading (FSO) vessels are recognized as one source of VOCs emissions. This study investigated the physical factors used to estimate the emission of VOCs from an FSO based on wave height, ambient temperature, storage temperature, storage quantity, Reid vapor pressure (RVP), and daily incoming rate. Daily data on the natural gas liquids were collected on the FSO. A second-order multiple linear regression (MLR) with interaction effects was used to analyze the relationship between the studied physical factors and VOC venting volumes. The set of relevant physical factors and interaction effects that produced the maximum adjusted coefficient of determination was selected. The significant factors and interaction effects were investigated based on a t-test at a significance level of 0.05. The results showed that the significant factors for estimation of the venting volume, corresponding to VOCs emissions, were wave height, storage temperature (which was related to the daily incoming rate), and RVP. Venting volume was negatively related to storage temperature, especially when the storage temperature was low, and wave height was positively related to venting volume when the RVP was high. The interaction effect showed that wave height was important when RVP was high and the second-order MLR showed that the storage temperature was important when it was low.

Keywords: floating storage and offloading (FSO); interaction effect; second-order multiple linear regression; volatile organic compounds (VOCs) emission

*Corresponding author: E-mail: ecpwk@ku.ac.th
<https://doi.org/10.55003/cast.2024.261920>

Copyright © 2024 by King Mongkut's Institute of Technology Ladkrabang, Thailand. This is an open access article under the CC BY-NC-ND license (<http://creativecommons.org/licenses/by-nc-nd/4.0/>).

1. Introduction

Natural gas liquids (NGLs) are condensable hydrocarbons that are from the same family of molecules as crude oil and natural gas and are composed mainly of carbon and hydrogen. NGLs are used in various fields including the petrochemical industry, cooking, vehicle fuel, and blended substances industries (U.S. Energy Information Administration, 2012). Following successful offshore petroleum extraction, natural gas (NG) is sent onshore for production processing at a central processing platform while NGLs are delivered via a subsea pipeline and stored in marine vessels called floating storage and offloading (FSO). NGLs are accumulated and stored in the FSO to a desired quantity prior to offloading to other receiving FSOs.

In the gulf of Thailand, the storage capacities of the FSOs vary in the range of 600,000-1,000,000 barrels (approximately 95,000 - 159,000 m³). When NGLs are stored in an FSO, volatile organic compound (VOC) vapors are simultaneously generated inside the vessel. Depending on the tank design rules and operational practices, the evaporating gases, mainly composed of VOCs, are vented into the atmosphere to prevent tank deformation from the increasing internal pressure (Ennis, 2006). The vented gas, containing a substantial percentage of VOCs, is transferred through an automatically operated vent valve and eventually released via a vent stack located on the main deck of the FSO (Virdi et al., 2021). The released VOCs can have adverse impact on human health and the environment; they often have strong odors, and can cause eye, nose and throat irritation, headaches, nosebleeds, fatigue, nausea, and dizziness. Exposure to very high levels of VOCs can possibly cause damage to the liver, kidneys, and central nervous system, while some VOCs, such as chloroform, formaldehyde, and benzene, are classified as carcinogens for humans (Fiedler et al., 2005). Additionally, VOCs play an important role in the formation of photochemical smog which is considered a secondary air pollutant (Shao et al., 2020). Other studies reported that the rate of VOC emission from an FSO depends on several physical factors including wave height, ambient temperature, storage temperature, storage quantity, Reid vapor pressure (RVP), and the NGL incoming rate (Rudd & Hill, 2001; Lang et al., 2017; Hu et al., 2020). As the storage temperature increases, energy is transferred to the liquid and stored in the form of the kinetic energy of molecules, inducing molecular transition into the vapor form and leading to an increase in the vapor pressure and VOC emissions. Some reports in the literature showed that in chamber tests, as the temperature was increased from 15°C to 30°C, VOC emissions increased by 1.5 to 129 times (Lin et al., 2009; Yang et al., 2017; Hu et al., 2020). The RVP, which indicates vaporization capability, is a parameter used to measure volatility under ambient conditions. A high value of RVP for the storage volume led to an increase in the level of evaporative emissions, corresponding to a high VOC venting volume (Seekramon, 2015). Some studies found that high levels of RVP, storage quantity, temperature inversion, and a low wind speed above the vent stack, resulted in an increase in the VOC emission rate (Chaiklieng et al., 2019; Deligiannis et al., 2016). Furthermore, the incoming rate of NGLs and the wave height (which can cause turbulence in the storage tank), resulting in high VOC emissions (Rudd and Hill, 2001; Stricklin, 2014; Deligiannis et al., 2016; Saikomol et al., 2019).

Although several studies have described the significant factors contributing to VOC emissions in the petroleum industry, most of these studies focused on production plants and onshore tank farms (Huang et al., 2018; Mo et al., 2021). However, an FSO has some distinguishing factors that differ from onshore facilities and possibly affect VOC emissions, such as wave height, causing turbulence of NGLs inside the tank. Additionally, most

studies described the effect of individual factors on VOC emissions and did not integrate such factors. There have been limited studies on the integration of the relevant factors affecting VOC emissions from FSOs.

Hence, this study investigated the relationship between combinations of various physical factors and VOC emissions from FSO vent stacks. These factors consisted of wave height, ambient temperature, storage temperature, storage quantity, RVP, and daily incoming rate. A second-order multiple linear regression (MLR) with interaction effects was used to analyze the relationships between the relevant physical factors and the VOC venting volume. This MLR can be used to estimate the VOC emissions released from the vent stack that may affect the workforce on the main deck of the FSO.

2. Materials and Methods

Initially, data were gathered on venting volumes of gases mainly composed of VOCs and physical factors affecting the venting volume (wave height, ambient temperature, storage temperature, storage quantity, RVP, and daily incoming rate). Then, outliers were removed to maintain reliability. After that, the relationship between venting volume and the physical factors was investigated using a second-order MLR with interaction effects. Next, significant terms in the relationship were determined based on a statistical t-test. Finally, the effects of relevant factors and interaction effects were determined. The details of each step are described as follows.

2.1 Data gathering and screening

The data used in this study consisted of the venting volumes and the physical factors potentially affecting the venting volumes (wave height, ambient temperature, storage temperature, storage quantity, RVP, and daily incoming rate). The wave height data were collected 100 times a day using a wave buoy (Fugro, Norway). In total, 33 out of 100 datapoints which were in the middle range were averaged and reported daily. Ambient temperatures were measured using a temperature sensor (PT100; SMA Solar Technology; Germany). The storage temperature and storage quantity were measured using temperature sensors and radar beams, respectively, with a tank monitoring system (Kongsberg GL-300; Norway). The daily incoming rate was determined as the difference between storage quantities on consecutive days. The RVP of NGL samples, defined as the absolute vapor pressure of the liquid at 37.8°C (100°F), was determined based on the ASTM-D323 test method, using a Holler Bomb Test (Koehler Instruments; USA). The venting volumes were measured using an ultrasonic flare gas flow meter (GF868; GE; USA), installed on the vent stack of the FSO. All the data were consistently collected daily throughout the year. The data screening was done by identifying outliers for all physical factors and venting volumes to control data quality. Some venting volume data were lower than usual due to closure of the vent stack during squalls and lightning episodes. Consequently, the data based on venting volumes which were less than 90,000 ft³ per day were excluded from this study. In total, the data from 326 days were used.

2.2 Second-order multiple linear regression with interaction effects

MLR was used to determine the relationships between the independent variables (wave height, ambient temperature, storage temperature, storage quantity, RVP, and daily incoming rate) and the dependent variable (venting volume). Since the effect of each

independent variable may not be constant, this study used a second-order MLR with interaction effects. With the second-order MLR, the effect of each independent variable could change when the value of that variable (physical factor) changed. With the interaction effect, the effect of each independent variable could change when the value of another independent variable changed. The equation for the second-order MLR with interaction effects is provided as equation (1) (Cho and Lee, 2018; Jia et al., 2020):

$$Y = a + \sum_{i=1}^n b_i x_i + \sum_{i=1}^n \sum_{j=i}^n c_{ij} x_i x_j \quad (1)$$

where Y is the modeled venting volume, a , b_i , and c_{ij} are constants, n is the number of factors, and x_i and x_j are the values of the i^{th} and j^{th} factors, respectively.

2.3 Selection of terms and measurement of accuracy

To exclude any unnecessary terms from the MLR, the adjusted coefficient of determination (adjusted R^2) was calculated to determine the usefulness of each term. The adjusted R^2 was calculated as shown in equation (2) (Akbarian et al., 2022; Pham, 2019):

$$R_{adj}^2 = 1 - (1 - R^2) \left(\frac{n-1}{n-p-1} \right) \quad (2)$$

where R_{adj}^2 is the adjusted coefficient of determination (adjusted R^2), R^2 is the coefficient of determination, n is the sample size, and p is the number of predictors (independent variables and interaction effects).

The selection of physical factors and interaction effects was done by maximizing the adjusted R^2 . In other words, the terms which did not improve the value of the adjusted R^2 were removed from the MLR. After maximizing the adjusted R^2 , the accuracy of the MLR was evaluated based on the root mean squared error (RMSE) as shown in equation (3) and coefficient of determination (R^2).

$$RMSE = \sqrt{\frac{1}{n} \sum_{i=1}^n (o_i - e_i)^2} \quad (3)$$

where $RMSE$ was the root mean squared error, n was the count of data, o_i was the i^{th} observed data, and e_i was the i^{th} modeled data. RMSE indicates the difference between the observed and calculated venting volumes, whereas R^2 indicates the proportion of the variance of the venting volume that the MLR can explain.

2.4 Significance test and investigation of effects of factors and interactions

A t-test was conducted to determine the significance of each term in the MLR (Cho and Lee, 2018). The null hypothesis of the test was that the coefficient of each term was 0, which meant that each physical factor or interaction effect did not affect the venting volume. In this study, the test was done at a significance level of 0.05. In other words, the effect of each factor or interaction effect was considered significant when $p\text{-value} < 0.05$. After the test, the effects of significant factors and interaction effects were determined based on scatter plots between the significant factors and the venting volume. From the scatter plot, it could be seen whether the venting volume was positively or negatively related to each

factor and whether the effect of each factor was constant or varied depending upon the conditions.

3. Results and Discussion

3.1 Relationship between venting volume and physical factors

The data screening identified that the venting volume on 40 days was less than 90,000 ft³. Consequently, the data on those 40 days were excluded from this study regarding weather conditions and maintenance of the vent stack (as described in Section 2.1). In total, the data from 326 days were used in this study. Table 1 summarizes the values of physical factors during the study period (after screening). The average venting volume was 210,984 ft³ with a standard deviation of 68,555 ft³. The high standard deviation suggested that the venting volume had high variability. The average ambient air temperature was 28.4°C with a standard deviation of 0.9°C; overall, the air temperature was higher and had less variability than similar data from other studies (Stricklin, 2014; Gjesteland et al., 2019; Hu et al., 2020). The RVP value exhibited low variability because the NGL composition of each batch was consistent.

The set of terms in the MLR that produced the highest value of the adjusted R², together with the coefficients of these terms and the results of the t-test, are shown in Table 2. The significant terms for the calculation of the venting volume were: 1) wave height, 2) storage temperature, 3) interaction effect between wave height and RVP, and 4) square of storage temperature. Therefore, the significant factors for estimation of venting volume were wave height, storage temperature and RVP. Considering the coefficients, the venting volume was high when the wave height was high and the storage temperature was low. However, the importance of these factors depends on the conditions (the values of physical factors). The importance of wave height depends on the value of RVP and the importance of storage temperature depends on its value. The effects of wave height and RVP were consistent with other studies (Rudd & Hill, 2001; Stricklin, 2014; Deligiannis et al., 2016). However, the effect of storage temperature in our study was different from many studies (Rudd & Hill, 2001; Stricklin, 2014; Deligiannis et al., 2016), because the storage temperature in the current study was affected by the daily incoming rate, which affected the venting volume (discussed later in Section 3.3.1).

The comparison between the observed and modeled venting volumes is shown in Figure 1. The modeled venting volume varied between 110,395 ft³ and 453,885 ft³ with an average of 210,984 ft³ and a standard deviation of 40,120 ft³. The MLR explained 32% of the variance of the venting volume ($R^2 = 0.320$) and the RMSE was 54,723 ft³. The venting volume was high during September–December (days 274–366) because of the influence of the monsoon season, leading to increasing wave heights.

Table 1. Summarized data of physical factors after screening

Statistic	Wave Height (m)	Ambient Air Temperature (°C)	Storage Temperature (°C)	Storage Quantity (bbl)	RVP (psi)	Daily Incoming Rate (bbl)	Venting Volume (ft ³)
Mean	1.1	28.4	29.4	492,012	12.1	43,163	210,984
Standard deviation	0.7	0.9	0.6	94,562	0.3	7,135	68,555
Maximum	3.8	31	31.1	733,387	13.5	61,164	436,548
Minimum	0.2	25	28.3	303,557	11.4	17,010	94,052

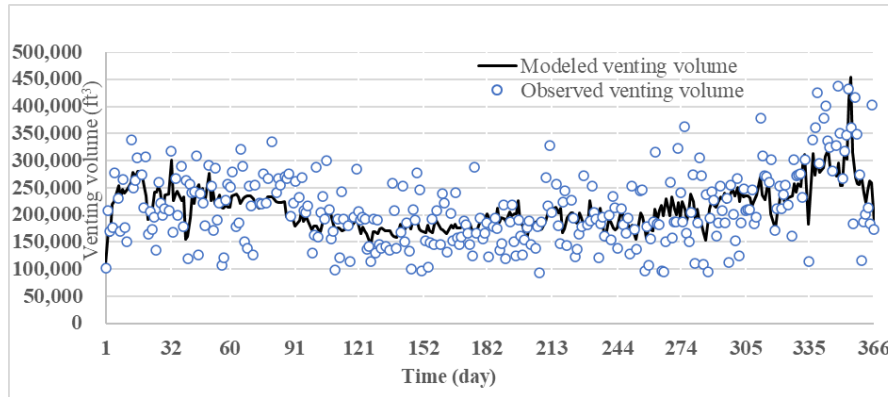


Figure 1. Observed and modeled venting volume from FSO

3.2 Significant physical factors

Since the significant terms in the MLR were 1) wave height, 2) storage temperature, 3) interaction effect between wave height and RVP, and 4) the square of storage temperature (Table 2), the significant physical factors were wave height, storage temperature, and RVP. However, since the storage temperature was influenced by the daily incoming rate, the daily incoming rate is also discussed in this section.

3.2.1 Storage temperature and daily incoming rate

The plot between storage temperature and venting volume is shown in Figure 2, indicating that the venting volume was high when the storage temperature was low. However, at high storage temperature, the venting volume appeared to be less associated with the storage temperature. This result was contrary to the findings from several other studies (Stricklin, 2014; Deligiannis et al., 2016; Hu et al., 2020). Theoretically, venting volume increases with increasing temperature because increased energy leads to greater movement of the liquid molecules inside the tank, which causes evaporation. However, in the current study, the venting volume was high when the storage temperature was low because the storage temperature was related to the daily incoming rate. According to the Pearson's correlation coefficient values between each pair of variables in Table 3, when the daily incoming rate was high, the storage temperature was low because the FSO incoming line was in direct contact with the subsurface seawater, while the venting volume was high because the daily incoming rate contributed to turbulence inside the tanks (Stricklin, 2014; Deligiannis et al., 2016). On the other hand, when the daily incoming rate was low, the storage temperature was high due to less incoming low temperature NGLs from the subsurface seawater, while the venting volume was low due to less turbulence inside the tanks (Rudd and Hill, 2001; Stricklin, 2014; Deligiannis et al., 2016; Yanowitz & McCormick, 2016; Hu et al., 2020; Gorokhovski & Oruganti, 2022; Zhang et al., 2022). Therefore, the storage temperature in this study could represent the effect of the daily incoming rate, which had an impact on the venting volume.

Table 2. Set of terms in MLR between physical factors and venting volumes providing highest value of adjusted R^2

Term	Coefficient	Standard Error	T-Statistic	p-Value
Intercept (ft ³)	20305955	7195253	2.82	0.005
Wave height (m)	-917882	225828.9	-4.06	<0.001*
Storage temperature (°C)	-1371979	467375	-2.94	0.004*
Daily incoming rate (bbl)	50.94174	40.31464	1.26	0.207
Storage temperature (°C) × Daily incoming rate (bbl)	-2.06136	1.46234	-1.41	0.16
Storage temperature (°C) × Ambient air temperature (°C)	-8736.81	5617.035	-1.56	0.121
Daily incoming Rate (bbl) × Wave height (m)	-1.00821	0.765968	-1.32	0.189
Daily incoming Rate (bbl) × Ambient air temperature (°C)	0.846988	0.742236	1.14	0.255
Daily incoming Rate (bbl) × RVP (psi)	-0.91399	0.51592	-1.77	0.077
Wave height (m) × Ambient air temperature (°C)	6276.615	5130.039	1.22	0.222
Wave height (m) × Storage quantity (bbl)	0.072509	0.047946	1.51	0.131
Wave height (m) × RVP (psi)	62090.83	15194.44	4.09	<0.001*
Storage temperature (°C) × Storage temperature (°C)	28052.72	8124.042	3.45	0.001*
Ambient air temperature (°C) × Ambient air temperature (°C)	3915.422	2826.716	1.39	0.167
Storage quantity (bbl) × Storage quantity (bbl)	-17.4598	6.18721×10 ⁻⁸	-1.69	0.092

* p-value<0.05 (significant)

Table 3. Pearson's correlation coefficient values between each pair of variables

Variable	Wave Height	Ambient Air Temperature	Storage Temperature	Storage Quantity	Daily Incoming Rate	RVP	Venting Volume
Wave height							
Ambient air temperature	-0.252*						
Storage Temperature	-0.394*	0.573*					
Storage quantity	0.044	-0.083	-0.217*				
Daily incoming rate	0.119*	-0.299*	-0.229*	0.216*			
RVP	-0.003	0.119*	0.133*	0.017	-0.051		
Venting volume	0.257*	-0.216*	-0.421*	0.104	0.273*	0.132*	

* Indicates that the correlations are significant according to the t-test at the 0.05 significance level.

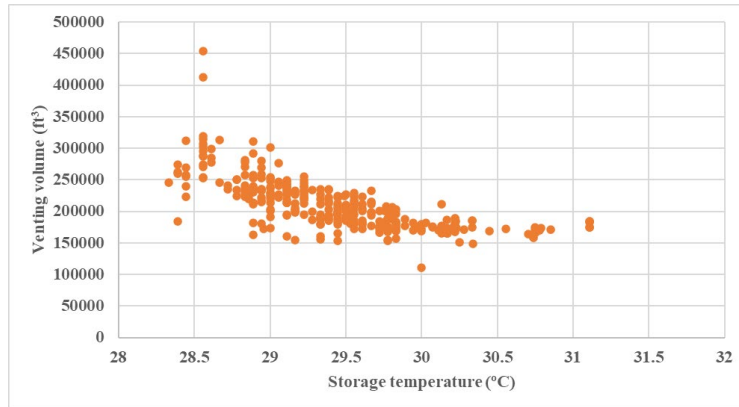


Figure 2. Scatter plot between storage temperature and venting volume

3.2.2 Wave height and RVP

The scatter plot between wave height and venting volume under different ranges of RVP is shown in Figure 3. The venting volume had a positive relationship with the wave height when the RVP was high. However, the relationship was weak when the RVP was low. At a low RVP (≤ 11.9 psi), the venting volume was not correlated with the wave height, while at an intermediate RVP (11.9-12.3 psi), the venting volume was slightly positively correlated with the wave height, and at a high RVP (> 12.3 psi) the venting volume was clearly positively correlated with the wave height. These results were due to the wave height leading to liquid movement, causing turbulence in the vessels, and generating VOC emissions. This finding was consistent with other studies (Stricklin, 2014; Hu et al., 2020). Furthermore, a high RVP enhanced evaporation of VOCs, leading to a high venting volume. This finding aligned with several other studies (Rudd and Hill, 2001; Stricklin, 2014; Deligiannis et al., 2016; Gjesteland et al., 2017).

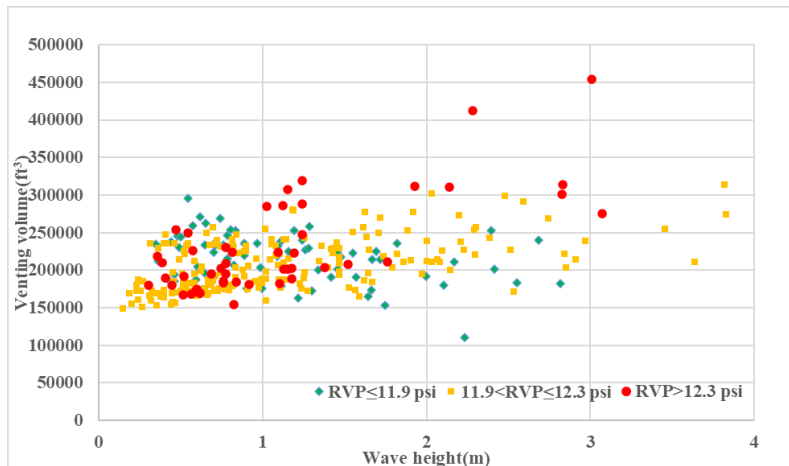


Figure 3. Scatter plot between wave height and venting volume for different ranges of RVP

4. Conclusions

This research investigated the relevant physical factors for estimation of VOC emissions from an FSO in a tropical region, based on the wave height, ambient temperature, storage temperature, storage quantity, RVP, and daily incoming rate. The average daily venting volume was 210,984 ft³. The estimation of venting volume was based on a second-order MLR with interaction effects. The set of terms (physical factors and interaction effects) used in the MLR was the one that produced the highest adjusted R² value, with a t-test used to determine the significance of each term. Significant physical factors that were important in the estimation of the venting volume were wave height, storage temperature, and RVP. The MLR with the selected terms accounted for 32.0% of the variance of the venting volume (R² = 0.320), with an RMSE of 54,723 ft³. Venting volume was negatively related to storage temperature, especially when storage temperature was low. The reason for this was that storage temperature was reflective of daily incoming rate, which had an impact on venting volume. When the daily incoming rate was high, the high volume of NGLs flowing through the subsurface pipeline resulted in a low storage temperature inside the tanks and the venting volume was high because the daily incoming rate contributed to turbulence inside the tanks. However, at high storage temperature, venting volume appeared to be less associated with storage temperature. Wave height was positively related with venting volume when RVP was high because the wave height led to liquid movement; however, the relationship was weak when RVP was low. The results from this study can be applied to estimate the venting volumes and VOC emissions from an FSO, which tended to be high when storage temperature was low and wave height and RVP were high. However, this research did not quantitatively determine the optimum condition for FSO venting operation to reduce exposure on the main deck. Nevertheless, the MLR obtained from this study can be further applied to evaluate and manage the health risks associated with exposure to VOCs from an FSO.

5. Acknowledgements

English editing assistance was provided by the Kasetsart University Research and Development Institute (KURDI), Bangkok, Thailand.

6. Conflicts of Interest

There is no conflicts of interest.

ORCID

Chalor Jarusutthirak  <https://orcid.org/0000-0001-7214-6744>

Pawee Klongvessa  <https://orcid.org/0000-0003-2907-3978>

References

Akbarian, H., Jalali, F. M., Gheibi, M., Hajiaghaei-Keshteli, M., Akrami, M., & Sarmah, A. K., (2022). A sustainable decision support system for soil bioremediation of toluene incorporating UN sustainable development goals. *Environmental Pollution*, 307, Article 119587. <https://doi.org/10.1016/j.envpol.2022.119587>.

- Chaiklieng, S., Suggaravetsiri, P., & Autrup, H. (2019). Risk assessment on benzene exposure among gasoline station workers. *International Journal of Environmental Research and Public Health*, 16(14), Article 2545. <https://doi.org/10.3390/ijerph16142545>
- Cho, J. H., & Lee, J. H. (2018). Multiple linear regression models for predicting nonpoint-source pollutant discharge from a highland agricultural region. *Water*, 10(9), Article 1156. <https://doi.org/10.3390/w10091156>
- Deligiannis, P., Zouridis, P., & Galis, A. (2016). *VOC emissions assessment from the cargo area of tanker vessels*. https://www.researchgate.net/publication/303813492_VOC_EMISSIONS_ASSESSMENT_FROM_THE_CARGO_AREA_OF_TANKER_VESSELS.
- Ennis, T. (2006). *Pressure relief considerations for low-pressure (atmospheric) storage tanks*. <https://www.icheme.org/media/9850/xix-paper-63.pdf>
- Fiedler, N., Laumbach, R., Kelly-McNeil, K., Liroy, P., Fan, Z.H., Zhang, J., Ottenweller, J., Ohman-Strickland, P., & Kipen, H. (2005). Health effects of a mixture of indoor air volatile organics, their ozone oxidation products, and stress. *Environmental Health Perspectives*, 113(11), 1542-1548. <https://doi.org/10.1289/ehp.8132>
- Gjesteland, I., Hollund, B. E., Kirkeleit, J., Daling, P., & Bråtveit, M. (2017). Oil spill field trial at sea: measurements of benzene exposure. *Annals of Work Exposures and Health*, 61(6), 692-699. <https://doi.org/10.1093/annweh/wxx036>
- Gjesteland, I., Hollund, B. E., Kirkeleit, J., Daling, P. S., Sørheim, K. R., & Bråtveit, M. (2019). Determinants of airborne benzene evaporating from fresh crude oils released into seawater. *Marine Pollution Bulletin*, 140, 395-402. <https://doi.org/10.1016/j.marpolbul.2018.12.045>
- Gorokhovski, M. A., & Oruganti, S. K. (2022). Stochastic models for the droplet motion and evaporation in under-resolved turbulent flows at a large Reynolds number. *Journal of Fluid Mechanics*, 932, Article A18. <https://doi.org/10.1017/jfm.2021.916>
- Hu, G., Butler, J., Littlejohns, J., Wang, Q., & Li, G. (2020). Simulation of cargo VOC emissions from petroleum tankers in transit in Canadian waters. *Engineering Applications of Computational Fluid Mechanics*, 14(1), 522-533. <https://doi.org/10.1080/19942060.2020.1728386>
- Huang, C., Hu, Q., Wang, H., Qiao, L., Jing, S., Wang, H., Zhou, M., Zhu, S., Ma, Y., Lou, S., Li, L., Tao, S., Li, Y., & Lou, D. (2018). Emission factors of particulate and gaseous compounds from a large cargo vessel operated under real-world conditions. *Environmental Pollution*, 242(Part A), 667-674. <https://doi.org/10.1016/j.envpol.2018.07.036>
- Jia, Z., Wang, J., Zhou, X., Zhou, Y., Li, Y., Li, B., & Zhou, S. (2020). Identification of the sources and influencing factors of potentially toxic elements accumulation in the soil from a typical karst region in Guangxi, Southwest China. *Environmental Pollution*, 256, Article 113505. <https://doi.org/10.1016/j.envpol.2019.113505>
- Lang, J., Zhou, Y., Chen, D., Xing, X., Wei, L., Wang, X., Zhao, N., Zhang, Y., Guo, X., Han, L., & Cheng, S. (2017). Investigating the contribution of shipping emissions to atmospheric PM_{2.5} using a combined source apportionment approach. *Environmental Pollution*, 229, 557-566. <https://doi.org/10.1016/j.envpol.2017.06.087>
- Lin, C.-C., Yu, K.-P., Zhao, P., & Lee, G. W.-M. (2009). Evaluation of impact factors on VOC emissions and concentrations from wooden flooring based on chamber tests. *Building and Environment*, 44(3), 525-533. <https://doi.org/10.1016/j.buildenv.2008.04.015>
- Mo, Z., Lu, S., & Shao, M. (2021). Volatile organic compound (VOC) emissions and health risk assessment in paint and coatings industry in the Yangtze River Delta, China.

- Environmental Pollution*, 269, Article 115740. <https://doi.org/10.1016/j.envpol.2020.115740>
- Pham, H. (2019). A new criterion for model selection. *Mathematics*, 7(12), Article 1215. <https://doi.org/10.3390/math7121215>
- Rudd, H. J., & Hill, N. A. (2001). *Measures to reduce emissions of VOCs during loading and unloading of ships in the EU*. <http://ec.europa.eu/environment/archives/air/pdf/vocloading.pdf>
- Saikomol, S., Thepanondh, S., Laowagul, W. (2019). Emission losses and dispersion of volatile organic compounds from tank farm of petroleum refinery complex. *Journal of Environmental Health Science and Engineering*, 17(2), 561-570. <https://doi.org/10.1007/s40201-019-00370-1>
- Seekramon, C. (2015). *Emission of volatile organic compounds from natural gas liquid tank vessel*. [unpublished MSc. Thesis]. Mahidol University.
- Shao, P., Xu, X., Zhang, X., Xu, J., Wang, Y., & Ma, Z. (2020). Impact of volatile organic compounds and photochemical activities on particulate matters during a high ozone episode at urban, suburb and regional background stations in Beijing. *Atmospheric Environment*, 236, Article 117629. <https://doi.org/10.1016/j.atmosenv.2020.117629>
- Stricklin, E. (2014). *Evaporation loss measurement from storage tanks*. <https://technokontrol.com/pdf/evaporation/evaporation-loss-measurement.pdf>.
- U.S. Energy Information Administration. (2012, April 20). *What are natural gas liquids and how are they used?* <https://www.eia.gov/todayinenergy/detail.php?id=5930>.
- Virdi, S. S., Lee, L. Y., Li, C., & Dev, A. K. (2021). Simulation of VOC emission during loading operations in a crude oil tanker. *The International Journal of Maritime Engineering*, 163(Part A1), A1-A16. <https://doi.org/10.5750/ijme.v163iA1.1>
- Yang, T., Zhang, P., Xu, B., & Xiong, J. (2017). Predicting VOC emissions from materials in vehicle cabins: determination of the key parameters and the influence of environmental factors. *International Journal of Heat and Mass Transfer*, 110, 671-679. <https://doi.org/10.1016/j.ijheatmasstransfer.2017.03.049>
- Yanowitz, J., & McCormick, R. (2016). Review: fuel volatility standards and spark-ignition vehicle driveability. *SAE International Journal of Fuels and Lubricants*, 9(2), 408-429. <https://doi.org/10.4271/2016-01-9072>
- Zhang, Y., Chen, F., Jia, M., He, Z., & Yi, P. (2022). Molecular dynamics investigation of the vaporization characteristics of n-alkane blended fuels under different ambient conditions. *AIP Advances*, 12, Article 075309. <https://doi.org/10.1063/5.0098054>